Reaction mechanism populating $^{12}C+^{16}O$ breakup states in ^{28}Si

N. Curtis,* M. Shawcross, and W. N. Catford
School of Physics and Chemistry, University of Surrey, Guildford, Surrey GU2 7XH, United Kingdom

B. R. Fulton, N. M. Clarke, S. J. Hall, and J. T. Murgatroyd
School of Physics and Astronomy, University of Birmingham, Edgbaston, Birmingham B15 2TT, United Kingdom

S. P. G. Chappell,† R. L. Cowin, G. Dillon, and D. L. Watson
Department of Physics, University of York, Heslington, York YO1 5DD, United Kingdom
(Received 27 September 1999; published 1 August 2000)

A measurement of the $^{12}C+^{16}O$ breakup of ^{28}Si following ^{24}Mg scattering from targets of carbon, lithium oxide, and beryllium has been performed. A study of the relative energy of the correlated ^{12}C and ^{16}O fragments has allowed the excitation energy of states in ^{28}Si to be determined. A comparison of the excitation energy spectra in ^{28}Si obtained from the three targets indicates that the same states are populated in the $^{12}C(^{24}Mg,^{12}C^{16}O)^{8}Be$, $^{7}Li(^{24}Mg,^{12}C^{16}O)t$, and $^{9}Be(^{24}Mg,^{12}C^{16}O)^{5}He$ reactions. The data support the hypothesis that the reaction mechanism populating the $^{12}C+^{16}O$ breakup states observed in these channels is α transfer, and rule out an alternative involving resonant, or ''doorway,'' states in the $^{12}C+^{24}Mg$ compound system.

PACS number(s): 25.70.Hi, 27.30.+t

I. INTRODUCTION

The near-symmetric fission of ^{28}Si excited states into ^{12}C and ^{16}O nuclei has been observed in a number of experiments in recent years [1–6]. The excitation energy spectrum of the parent ^{28}Si nucleus, obtained from a study of the relative energy of the correlated ^{12}C and ^{16}O fragments [7], is seen to display discrete peaks in both the $^{12}C(^{20}Ne,^{12}C^{16}O)^{4}He$ [4] and $^{12}C(^{24}Mg,^{12}C^{16}O)^{8}Be$ [1–3] reactions. Evidence for the $^{12}C+^{16}O$ breakup of ^{28}Si states has also been seen in the $^{16}O(^{16}O,^{12}C^{16}O)^{4}He$ reaction [6]. The ^{12}C and ^{16}O breakup of ^{28}Si may occur from states that are members of one or more highly deformed rotational bands, as is the case in the $^{12}C+^{12}C$ breakup of ^{24}Mg [8], and has been suggested to be the case in the $^{16}O+^{16}O$ breakup of ^{32}S [9]. The breakup states in ^{28}Si may also be expected to be closely related to the resonances seen in ^{12}C and ^{16}O scattering at or near Coulomb barrier energies, in analogy with the correspondence observed in the $^{12}C+^{12}C$ breakup of ^{24}Mg [10].

The Nilsson-Strutinsky calculations of Leander and Larsson [11] predict several minima in the potential energy surface for ^{28}Si, calculated as a function of spheroidal deformation parameters. In addition to the known oblate ground state well, secondary minima also appear at triaxial, prolate, and a second oblate deformation. Several quasistable configurations have also been found in the α-cluster model calculations of Zhang *et al.* [12], and a correspondence was noted between the oblate (ground state) and prolate configurations found in the Nilsson-Strutinsky work and those found in the α-cluster model calculations. The prolate structure seen in the α-cluster model work and associated with the prolate well in the Nilsson-Strutinsky calculations has a $^{12}C_{g.s.}+^{16}O_{g.s.}$ structure and it is suggested [12] that the higher members of the corresponding rotational band may be one of the configurations populated in the $^{12}C+^{16}O$ elastic scattering resonances [13,14]. This prolate well has also been suggested by Freer to be populated by the breakup states observed in the $^{12}C(^{24}Mg,^{12}C^{16}O)^{8}Be$ reaction [2]. However, this association relies on a tentative spin assignment for the breakup states and more definite assignments would be required to enable a full comparison between the experimental data and the rotational band predicted for the prolate α-cluster configuration.

As noted earlier, breakup states are observed in the $^{12}C(^{20}Ne,^{12}C^{16}O)^{4}He$ [4] and $^{12}C(^{24}Mg,^{12}C^{16}O)^{8}Be$ [1–3] reactions, although there does not appear to be an obvious overlap between the two sets. However, Bennett *et al.* have reported that no evidence is found for the sequential breakup of ^{28}Si following the inelastic scattering of a ^{28}Si beam in the $^{12}C(^{28}Si,^{12}C^{16}O)^{12}C$ reaction [5], and this suggests that particle transfer plays an important role in the formation of the breakup states observed. Using the model of Harvey [15], Bennett *et al.* [5] have shown that it is not possible for ^{28}Si in the (oblate) ground state configuration to breakup into ground state ^{12}C and ^{16}O fragments. In this case it is not possible for the individual nucleons to rearrange themselves from the single-particle shell model orbits of the ^{28}Si ground state to the single-particle orbits of the separate ^{12}C and ^{16}O fragments. The $^{12}C+^{16}O$ breakup of ^{28}Si is not forbidden by the Harvey model, however, following, for example, an α transfer onto a ^{24}Mg beam, as such a reaction is not restricted to populating the ^{28}Si ground state configuration. Indeed, the ^{28}Si states formed by combining ^{12}C and ^{16}O fragments in the Harvey model have a four-particle–four-hole character. The model can therefore account for the ob-

*Present address: Department of Physics, Florida State University, Tallahassee, FL 32306.

†Present address: Department of Nuclear Physics, University of Oxford, Keble Road, Oxford OX1 3RH, U.K.

servation of ^{28}Si breakup in experiments using ^{20}Ne and ^{24}Mg beams and the observed lack of breakup in the ^{12}C(^{28}Si,^{12}C^{16}O)^{12}C channel.

In this paper we report on an experiment performed to investigate the possible α-transfer mechanism populating the breakup states observed in the ^{12}C(^{24}Mg,^{12}C^{16}O)^{8}Be reaction. Studies of this channel and the ^{7}Li(^{24}Mg,^{12}C^{16}O)t and ^{9}Be(^{24}Mg,^{12}C^{16}O)^{5}He reactions have been performed, using targets of ^{12}C,^{7}Li, and ^{9}Be. The targets of ^{7}Li and ^{9}Be were chosen as these nuclei are known to exhibit strong $(\alpha+t)$ and $(\alpha+\alpha+n)$ ground state cluster structures, respectively (see, for example, Refs. [16,17]). They are therefore well suited to the study of α-transfer reactions. Experimentally, such a comparison between different targets is an attractive method of studying the reaction mechanism. In this work the interest centers specifically on the breakup states in ^{28}Si, and to ''tag'' their population requires the detection of the breakup fragments. With this extra requirement the measurement of a conventional angular distribution for the primary reaction becomes very difficult experimentally. In addition, the present approach automatically tests whether the ^{12}C target or the combined ^{12}C+^{24}Mg system has any special properties necessary to populate the breakup states.

II. EXPERIMENTAL DETAILS

The experiment employed a beam of 170 MeV ^{24}Mg ions, provided by the 14UD tandem accelerator of the Department of Nuclear Physics at the Australian National University. The beam was incident separately upon targets of nominally 380 μg cm^{-2} natural carbon, 300 μg cm^{-2} lithium oxide, and 350 μg cm^{-2} natural beryllium.

The lithium oxide target was produced by evaporation of the oxide onto a previously prepared thin carbon backing. The elemental composition of an identical target from the same production batch was analyzed using Rutherford back scattering (RBS) [18]. A beam of 1 MeV ^{1}H ions was provided by The University of Surrey Ion Beam Facility, with the scattered ^{1}H ions being detected at 165° in a silicon surface barrier detector. The RBS analysis revealed a composition approximately consistent with $LiCO_4$, with a total thickness of 385 μg cm^{-2} plus the 12 μg cm^{-2} carbon backing. The backing was clearly separated in the spectrum analysis. The remaining carbon was distributed uniformly through the target and is believed to be a consequence of the target fabrication process. The lithium thickness was 62 μg cm^{-2}. The RBS measurements are believed to have an absolute uncertainty of less than 20%.

Coincident ^{12}C and ^{16}O nuclei from the breakup of the excited ^{28}Si nucleus were detected in two gas-silicon-scintillator hybrid detector telescopes placed horizontally on either side of the beam axis and centred at laboratory angles of 16°. The first element of each hybrid telescope was a 50 mm deep longitudinal gas ionization chamber filled to 60 Torr with propane, which acted as a ΔE detector. Behind this was a position sensitive silicon strip detector, comprised of 16 independent horizontal strips fabricated onto a single 50 mm×50 mm silicon wafer, 500 microns thick. Each strip was 3 mm wide and position sensitive along its length. The silicon detector provided both position and energy information, and when used in conjunction with the gas detector also provided ΔE-E particle identification. A 50 mm ×50 mm CsI scintillator, 10 mm thick, was placed behind the silicon strip detector in order to veto light energetic particles (typically α particles) that passed through the silicon detectors. These light particles could otherwise be mistaken for heavy ion events if a heavy ion was stopped simultaneously within the gas detector. These telescopes are an extension of the gas-silicon hybrid detectors described previously by Curtis *et al.* [7]. The distance from the target to each silicon detector was 170 mm, and the angular acceptance of each telescope was 87 msr. The beam exposures for the carbon, lithium oxide, and beryllium targets were 0.19, 0.51, and 0.44 mC, respectively.

III. RESULTS AND DISCUSSION

Figure 1(a) shows the spectrum of the total summed energy ($E_{\rm tot}$) for the three final fragments from the ^{12}C(^{24}Mg,^{12}C^{16}O)^{8}Be reaction. The kinetic energy of the unobserved ^{8}Be was determined by applying momentum conservation between the ^{24}Mg beam particle and the two detected breakup fragments, assuming a three-body final state [7]. The peak labeled Q_{ggg} in Fig. 1(a) corresponds to events where all three exit channel particles are emitted in their ground states. The Q_{ggg} peak therefore appears at a total energy value equal to the beam energy plus the three-body Q value (Q_3) for the reaction (after allowances have been made for the average energy loss of the beam particle and breakup fragments in the target). For the ^{12}C(^{24}Mg,^{12}C^{16}O)^{8}Be reaction, $Q_3=-14.137$ MeV. In obtaining Fig. 1(a), a recoil mass of 8 units has been assumed. The justification for this comes from Fig. 2 which shows the missing energy and the missing momentum of the unobserved recoil particle. The recoil energy is deduced from the sum of the observed energies, whilst the momentum calculation relies on both the energy and position measurements. The quantity plotted on the horizontal axis is $P^2_{\rm recoil}/2$ and hence the Q_{ggg} events appear as a line with a slope given by $1/m_{\rm recoil}$, where $m_{\rm recoil}$ is the recoil mass. The intercept of this line on the vertical axis is equal to Q_3, the three-body Q value for the reaction. The diagonal solid line in Fig. 2 indicates the predicted Q_{ggg} locus for the ^{12}C(^{24}Mg,^{12}C^{16}O)^{8}Be reaction. The region of increased counts along this line, corresponding to events falling under the peak labeled Q_{ggg} in Fig. 1(a), indicate that these events are indeed associated with a mass 8 recoil. The events appearing at $E_{\rm tot}$ values less than that of the Q_{ggg} peak have a spectrum without any clear narrow peaks, suggesting that they are dominated by events where the assumption of a three-body exit channel does not hold.

After selecting events appearing in the Q_{ggg} peak in the $E_{\rm tot}$ spectrum the excitation energy in the excited ^{28}Si* nucleus may be determined by considering the relative energy of the ^{12}C and ^{16}O breakup fragments [7]. The excitation energy spectrum for the ^{12}C(^{24}Mg,^{12}C^{16}O)^{8}Be channel is shown in Fig. 3(a). In this spectrum a series of discrete peaks may be observed at excitation energies of approxi-

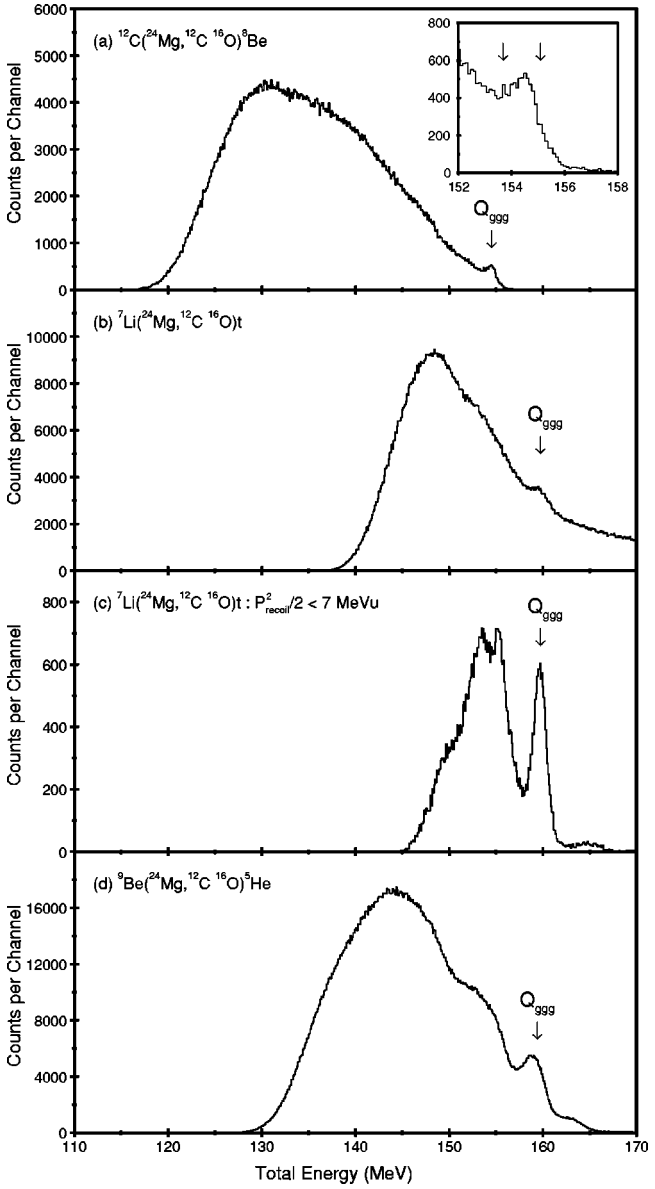

FIG. 1. Total energy spectra for $(^{24}Mg,^{12}C^{16}O)$ reactions on the carbon, lithium oxide, and beryllium targets. The inset to (a) shows the limits of the software gate used to filter the data. In (c), the spectrum for the lithium oxide target is shown with a restriction placed on the recoil momentum, as described in the text.

mately 28.0, 29.8, 30.5, 31.4, 33.4, and 34.5 MeV. The measured centroid energies are listed in Table I and compared to a previous measurement [3]. The dashed line in Fig. 3(a) indicates the predicted coincidence detection efficiency obtained from a Monte Carlo code that has been developed to simulate breakup reactions [10]. The peak detection efficiency is 15.7%. In this simulation an exponential fall-off has been assumed for the angular distribution of the initial scattering, and an isotropic distribution is assumed for the breakup of the ^{28}Si nucleus. At excitation energies below 26 MeV the spectrum is suppressed by the proximity to the Coulomb barrier between the breakup fragments. At high excitation energies there appears to be a reduction in detected events due to a real fall-off in cross section with excitation energy. The double differential cross section for the $^{12}C(^{24}Mg,^{12}C^{16}O)^{8}Be$ reaction, integrated over all excitations in ^{28}Si and averaged over the detector acceptances, is given in Table II and has a value of $d^2\sigma/d\Omega_1 d\Omega_2 = (0.41 \pm 0.05)$ mb sr^{-2}.

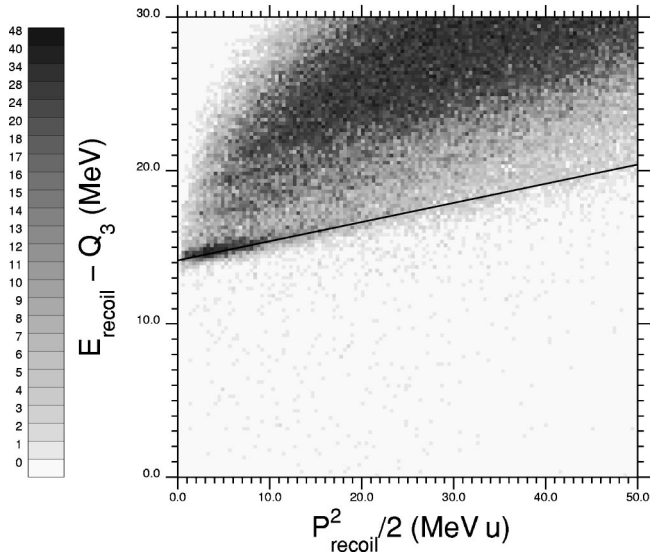

FIG. 2. Missing energy in the exit channel plotted against $p^2/2$, where p is the recoil momentum determined from momentum conservation assuming a three-body final state. The data were obtained for the $^{12}C+^{16}O$ breakup of ^{28}Si from the carbon target, and the diagonal solid line indicates the expected Q_{ggg} locus for the $^{12}C(^{24}Mg,^{12}C^{16}O)^{8}Be$ reaction.

During the analysis of the data shown in Fig. 3(a) it has been assumed that the detected ^{12}C and ^{16}O nuclei are fragments from the breakup of ^{28}Si. Of course, the same final state particles may be produced in both the $^{12}C(^{24}Mg,^{24}Mg^*)^{12}C, ^{24}Mg^* \rightarrow ^{16}O+^{8}Be$ and $^{12}C(^{24}Mg,^{20}Ne^*)^{16}O, ^{20}Ne^* \rightarrow ^{12}C+^{8}Be$ reactions. If such breakup occurred then the excitation energy spectrum reconstructed between the detected ^{16}O nucleus and the ^{8}Be recoil may show structure corresponding to breakup from specific excited states in ^{24}Mg, as reported by Murgatroyd *et al.* [19]. Similarly, structure may be observed in ^{20}Ne following $^{12}C+^{8}Be$ reconstruction. Figure 4 shows a two-dimensional plot of the excitation energy as calculated assuming $^{12}C+^{16}O$ breakup of ^{28}Si against that calculated assuming the $^{16}O+^{8}Be$ breakup of ^{24}Mg. Although it is possible to see vertical loci corresponding to the states seen in Fig. 3(a) in this plot, there is no evidence for horizontal loci (corresponding to $^{16}O+^{8}Be$ breakup) or diagonal loci (corresponding to the $^{12}C+^{8}Be$ channel). Therefore the $^{12}C+^{16}O$ excitation energy spectrum shown in Fig. 3(a) does not appear to contain contamination from ^{24}Mg or ^{20}Ne breakup. This is not surprising since in both of these possible contaminant channels the coincident detection of both a ^{12}C and an ^{16}O nucleus would require that one of these detected particles was a breakup fragment from the excited resonant nucleus and that the other was the recoiling target like nucleus, which will have a very low energy. For both of these reaction channels the energy of the recoil falls below the low-energy thresholds

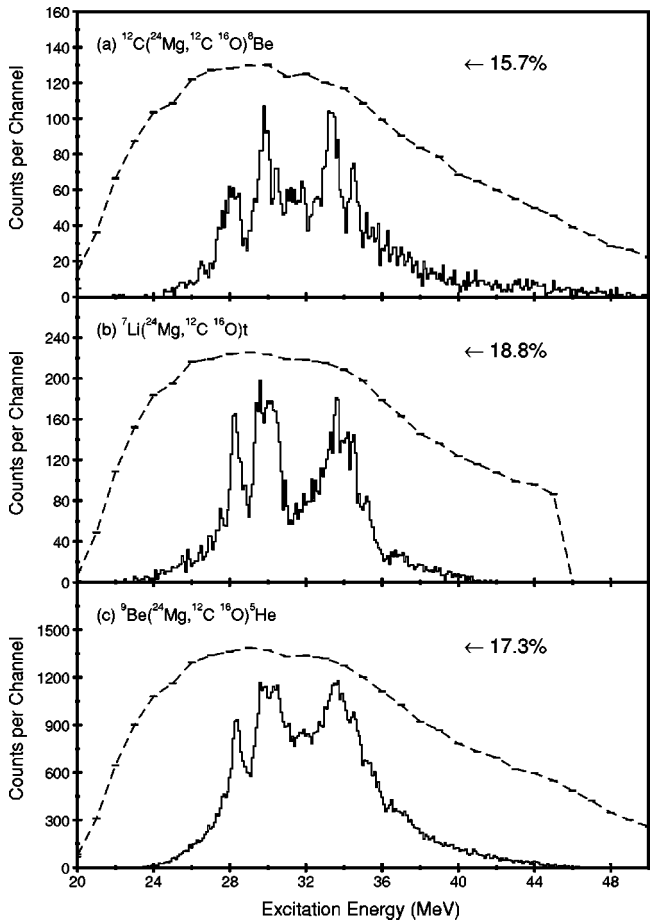

FIG. 3. Excitation energy spectra for the $^{12}C+^{16}O$ breakup of ^{28}Si from targets of (a) ^{12}C, (b) ^{7}Li, and (c) ^{9}Be. The Monte Carlo predicted efficiency profiles are indicated by the dashed lines.

of the detector telescopes (14 MeV for ^{12}C and 16 MeV for ^{16}O) over the angular range covered (7.6° to 24.4° in the laboratory).

Figure 1(b) shows a spectrum of the total summed energy ($E_{\rm tot}$) for the (^{24}Mg,^{12}C^{16}O) reaction on the $LiCO_4$ target reconstructed assuming a three-body final state and a mass 3 recoil. For the ^{7}Li(^{24}Mg,^{12}C^{16}O)t reaction, $Q_3=-9.239$ MeV. The peak labeled Q_{ggg} is thus consistent with the reaction of interest. However, due to the composite nature of the target, reactions involving the ^{12}C and ^{16}O target nuclei are also present in Fig. 1(b) and give rise to the high level of background underlying the Q_{ggg} peak. A clearer selection of the events of interest is achieved by comparing the missing energy and missing momentum of the unobserved recoil particle, as shown in Fig. 5. The predicted Q_{ggg} locus for the ^{7}Li(^{24}Mg,^{12}C ^{16}O)t channel is indicated by the diagonal solid line. The region of increased counts along this line, indicated by the bounded region, corresponds to the Q_{ggg} events of interest. The figure shows that for these events, $P^2_{\rm recoil}/2<7$ MeV u, corresponding to triton recoil energies less than $\sim$2.3 MeV. Figure 1(c) shows the $E_{\rm tot}$ spectrum with this additional requirement on the recoil momentum, in which the background underlying the $Q_{\rm ggg}$ peak is considerably reduced compared to that in Fig. 1(b) and reflects the true background level. Events falling within the bounded region of Fig. 5 were selected for subsequent analysis [equivalent to selecting the peak region in Fig. 1(c)]. The excitation energy spectrum thus obtained is shown in Fig. 3(b), where the dashed line again indicates the Monte Carlo predicted coincidence detection efficiency. Three distinct peaks may be observed at excitation energies of approximately 28.3, 29.9, and 33.8 MeV, and these centroids are compared in Table I with the energies observed for the ^{12}C target data. The double differential cross section for the ^{7}Li(^{24}Mg,^{12}C^{16}O)t channel, averaged over the detector acceptances is $d^2\sigma/d\Omega_1 d\Omega_2=(1.16\pm0.23)$ mb sr^{-2} (Table II). The RBS value for the lithium content of the target has been used. A study of the excitation energy reconstructed assuming $^{12}C+^{16}O$ breakup of ^{28}Si plotted against that assuming $^{16}O+t$ breakup of ^{19}F indicates that there is no ^{19}F or ^{15}N($^{12}C+t$) breakup contamination in Fig. 3(b). This analysis was similar to that shown in Fig. 4 for the ^{12}C target data.

Figure 1(d) shows the summed total energy ($E_{\rm tot}$) for the three final fragments from the ^{9}Be(^{24}Mg,^{12}C^{16}O)^{5}He reaction, for which $Q_3=-9.239$ MeV. The peak labeled Q_{ggg} again corresponds to events in which all three particles are emitted in the ground state. Note that, although the $E_{\rm tot}$ resolution is fundamentally limited by the width of the unbound ^{5}He ground state [$\Gamma=(0.68\pm0.03)$ MeV [20]], the limiting

TABLE I. Summary of the measured centroid energies of the states observed in the $^{12}C+^{16}O$ breakup of ^{28}Si. In the first column the results of a previous measurement by Curtis [3] are shown.

^{12}C(^{24}Mg,^{12}C^{16}O)^{8}Be Curtis	^{12}C(^{24}Mg,^{12}C^{16}O)^{8}Be present work	^{7}Li(^{24}Mg,^{12}C^{16}O)t present work	^{9}Be(^{24}Mg,^{12}C^{16}O)^{5}He present work
E_x (MeV)	E_x (MeV)	E_x (MeV)	E_x (MeV)
28.22±0.03	28.03±0.02	28.30±0.02	28.35±0.01
30.03±0.03	29.81±0.01	29.94±0.01	30.09±0.01
	30.48±0.01		
31.29±0.10	31.44±0.05		
33.43±0.04	33.39±0.01	33.79±0.02	33.77±0.01
	34.50±0.01		

TABLE II. Cross sections for the $^{12}C_{g.s.}+^{16}O_{g.s.}$ breakup of ^{28}Si. The double differential cross sections are given in terms of laboratory solid angle, and are directly measured quantities (averaged over the detector acceptances, and summed over all excitation energies in ^{28}Si). The total cross sections have had an efficiency correction applied, based on Monte Carlo simulations (and are summed over the excitation range 27–36 MeV in ^{28}Si). The errors labeled ''stat'' include an allowance for target-dependent effects in the efficiency corrections (see text).

Reaction Channel	$\frac{d^2\sigma}{d\Omega_1 d\Omega_2}$ (mb sr^{-2})	$\sigma(E_x=27-36$ MeV) (μb)
$^{12}C(^{24}Mg,^{12}C^{16}O)^{8}Be$	0.41 ± 0.05	$13.9\pm3.2_{stat}\pm4.2_{sys}$
$^{9}Be(^{24}Mg,^{12}C^{16}O)^{5}He$	1.41 ± 0.53	$37.6\pm13.6_{stat}\pm11.3_{sys}$
$^{7}Li(^{24}Mg,^{12}C^{16}O)t$	1.16 ± 0.23	$33.0\pm9.6_{stat}\pm9.9_{sys}$

factors in the case of all targets are actually the energy loss of the beam and fragments in the target, and the detector energy resolution. For example, these effects contribute approximately 900 keV to the width of the E_{tot} spectrum Q_{ggg} peak for the ^{9}Be target data. The excitation energy spectrum, discussed below, is unaffected by the recoil width. This is because the breakup of the ^{5}He recoil [or ^{8}Be in the case of the $^{12}C(^{24}Mg,^{12}C^{16}O)^{8}Be$ reaction] occurs sequentially after the production of the excited $^{28}Si^*$ nucleus, as indicated by the peak in the three-body Q-value spectrum. A plot of the recoil energy, obtained from energy conservation, against the missing momentum for the $^{9}Be(^{24}Mg,^{12}C^{16}O)^{5}He$ reaction is shown in Fig. 6. The predicted Q_{ggg} locus for this channel is indicated and an area of increased events is again observed in this region, indicating that these events are indeed associated with a recoil mass of 5 units.

It is interesting to note that in addition to the Q_{ggg} trajectory observed in Fig. 6 there is also a region of increased

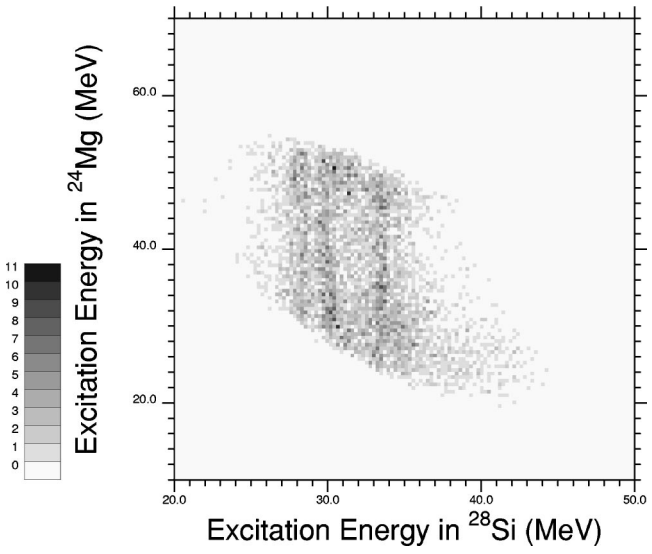

FIG. 4. Reconstructed excitation energy assuming $^{12}C+^{16}O$ breakup of ^{28}Si plotted against that calculated assuming $^{16}O+^{8}Be$ breakup of ^{24}Mg.

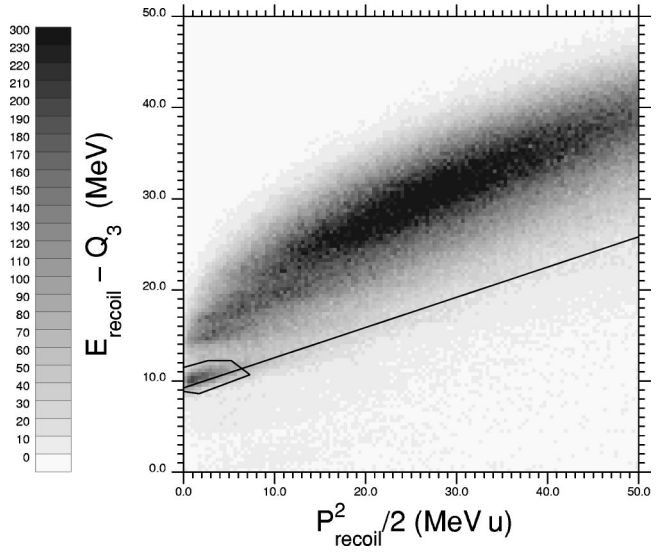

FIG. 5. As for Fig. 2, but for the lithium oxide target. The diagonal solid line indicates the expected Q_{ggg} locus for the $^{7}Li(^{24}Mg,^{12}C^{16}O)t$ reaction. The position of the software gate used to filter the data is also indicated.

events intercepting the y axis at $(E_{recoil}-Q_3)\approx5$ MeV. These events are identified as arising from the breakup of ^{29}Si via either the $^{9}Be(^{24}Mg,^{12}C^{17}O)^{4}He$ or $^{9}Be(^{24}Mg,^{13}C^{16}O)^{4}He$ reactions. Such events could be produced by either transfer or incomplete fusion. The particle identification information provided by the detector telescopes is limited to the fragment charge only, and it is therefore not possible to distinguish between isotopes such as ^{12}C and ^{13}C (or ^{16}O and ^{17}O). In addition, the similar three-body Q values for the $^{9}Be(^{24}Mg,^{12}C^{17}O)^{4}He$ ($Q_3=-4.201$ MeV) and $^{9}Be(^{24}Mg,^{13}C^{16}O)^{4}He$ ($Q_3=-3.398$ MeV) reactions means that it is not possible to

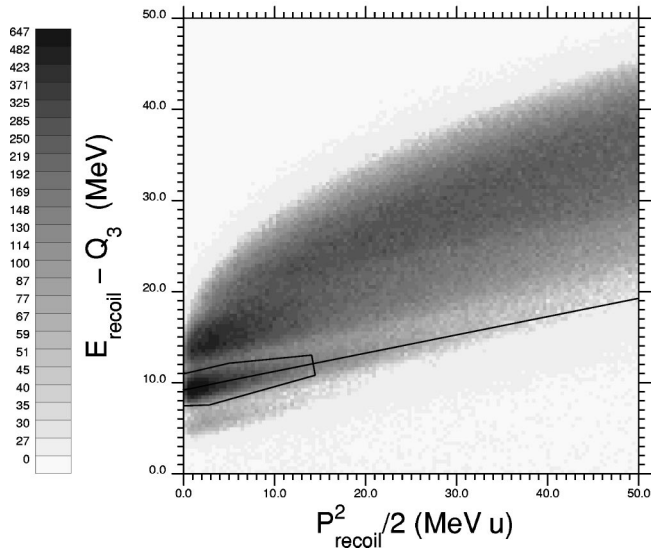

FIG. 6. As for Figs. 2 and 5, but for the beryllium target. The diagonal solid line indicates the expected Q_{ggg} locus for the $^{9}Be(^{24}Mg,^{12}C^{16}O)^{5}He$ reaction.

distinguish between these two channels and determine to what extent each is responsible for the region of increased events below the ^{9}Be(^{24}Mg,^{12}C^{16}O)^{5}He Q_{ggg} locus.

The excitation energy of the ^{28}Si* nucleus produced in the ^{9}Be(^{24}Mg,^{12}C^{16}O)^{5}He reaction, determined after gating on the Q_{ggg} locus seen in Fig. 6, is shown in Fig. 3(c). The predicted coincidence detection efficiency is also shown. Three distinct peaks are observed in this spectrum at excitation energies of 28.4, 30.1, and 33.8 MeV (Table I). These energies are similar to those measured for both the ^{12}C(^{24}Mg,^{12}C^{16}O)^{8}Be and ^{7}Li(^{24}Mg,^{12}C^{16}O)t reactions. The double differential cross section, averaged over the detector acceptances, is listed in Table II. As for the carbon and lithium oxide target data a study of the final state interactions in ^{21}Ne(^{16}O+^{5}He breakup) and ^{17}O(^{12}C+^{5}He breakup) via a plot analogous to Fig. 4 indicates that there is no background from these channels in the excitation energy spectrum for the ^{9}Be(^{24}Mg,^{12}C^{16}O)^{5}He reaction [Fig. 3(c)].

A comparison of the excitation energy spectra for the ^{12}C(^{24}Mg,^{12}C^{16}O)^{8}Be, ^{7}Li(^{24}Mg,^{12}C^{16}O)t, and ^{9}Be(^{24}Mg,^{12}C^{16}O)^{5}He reactions is given in Fig. 3 and strongly suggests that the same states are being populated in the different reactions. The data in Table I imply that the average difference in the measured centroids for the three clearest peaks is 175 keV, a typical value of the uncertainty generally noted in reconstructed excitation energy spectra obtained from breakup reactions of this kind.

In fact it is possible to improve the resolution of the ^{28}Si excitation energy spectra seen in Fig. 3 by restricting the data to exclude the lower energy ^{16}O fragments. The relevant ^{16}O energies span the range up to $\sim$125 MeV in the laboratory and the threshold was set to reject energies below $\sim$85 MeV (this is turn places restrictions on the ^{12}C fragment, as the energies of the two particles are correlated). The energy restriction is equivalent to placing a selection on the decay angle of the correlated fragments, so as to select forward going ^{16}O ions. Lee *et al.* [21] have previously noted that such a reduction in the range of decay angles is known to improve the excitation energy resolution obtainable. In Fig. 7(a) the excitation energy spectrum for the ^{12}C(^{24}Mg,^{12}C^{16}O)^{8}Be reaction, obtained following the ^{16}O fragment energy gating, is shown. The improvement in resolution when compared to the full data set [Fig. 3(a)] is clear, with peaks now being visible at excitation energies of approximately 26.5, 27.9, 28.4, 29.7, 30.5, 31.6, 32.3, 33.0, 33.5, and 34.4 MeV. The centroids and the measured widths of the peaks are listed in Table III. The gated spectrum for the ^{7}Li(^{24}Mg,^{12}C^{16}O)t channel is shown in Fig. 7(b). As for the carbon target data there is an improvement in the resolution when compared to the full data set, with peaks now being visible at excitation energies of approximately 28.1, 28.5, 29.5, 30.4, 31.6, 33.0, 33.7, and 34.4 MeV (Table III). In Fig. 7(c) the gated ^{9}Be(^{24}Mg,^{12}C^{16}O)^{5}He excitation energy spectrum is shown. Again an improvement in resolution is seen, although a large underlying background still remains below the peaks. The peak centroids and widths are listed in Table III. The dashed lines in Fig. 7 indicate the Monte Carlo predicted coincidence efficiencies taking into account the fragment energy restrictions discussed above.

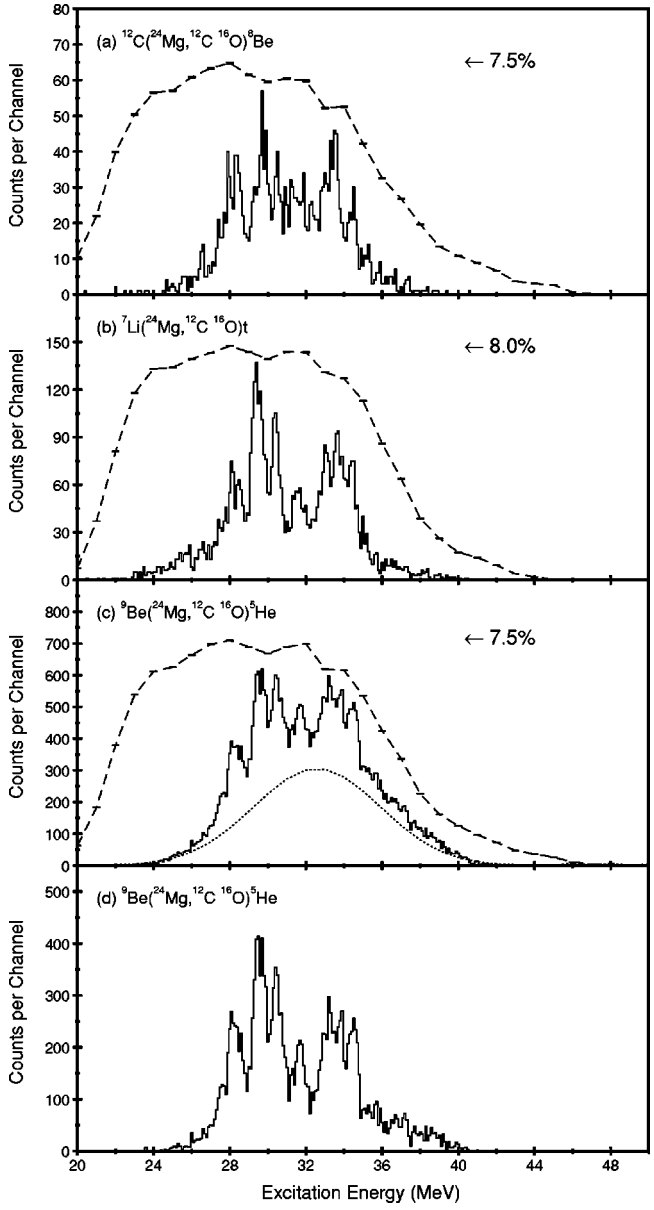

FIG. 7. Excitation energy spectra for the ^{12}C+^{16}O breakup of ^{28}Si obtained by restricting the ^{16}O fragment energy. The spectra are for targets of (a) ^{12}C, (b) ^{7}Li, (c) ^{9}Be, and (d) ^{9}Be with background subtraction. The Monte Carlo predicted efficiency profiles, taking into account the restriction on the ^{16}O fragment energy, are indicated by the dashed lines.

The dotted line in Fig. 7(c) corresponds to an estimate of the background included in the spectrum. This estimate was obtained by producing excitation energy spectra from data in the regions immediately above and below the Q_{ggg} peak in the total energy spectrum for this channel. These data derive from processes other than that of interest and must satisfy certain kinematic conditions in order to lie in this region of the total energy spectrum. They are well fitted in the excitation energy spectra by Gaussian distributions, with an average centroid of 32.6 MeV and a full width half maximum of 7.9 MeV. A Gaussian with these parameters is indicated by the dotted line in Fig. 7(c), with the area adjusted to match

TABLE III. Summary of the measured centroid energies and widths of the states observed in the $^{12}C+^{16}O$ breakup of ^{28}Si, obtained after gating on the energy of the ^{16}O fragment. The second list of ^{9}Be target centroids and widths corresponds to the background subtracted excitation energy spectrum.

^{12}C target		^{7}Li target		^{9}Be target		^{9}Be target (2)	
E_x (MeV)	ΔE (keV)	E_x (MeV)	ΔE (keV)	E_x (MeV)	ΔE (keV)	E_x (MeV)	ΔE (keV)
26.54±0.01	186±50						
27.94±0.01	220±27	28.11±0.01	24±22				
				28.22±0.01	812±31	28.22±0.01	918±24
28.40±0.01	347±37	28.51±0.01	279±35				
29.73±0.02	524±47	29.47±0.01	628±19	29.56±0.01	630±18	29.55±0.01	624±13
30.48±0.01	196±30	30.40±0.01	413±21	30.47±0.01	637±27	30.46±0.01	648±18
31.55±0.06	754±78	31.59±0.02	511±63	31.69±0.01	555±37	31.69±0.01	465±22
32.32±0.03	229±77						
32.96±0.03	301±57	33.02±0.02	430±44	33.25±0.02	1040±58	33.24±0.01	844±32
33.50±0.02	507±45	33.70±0.02	551±53	33.85±0.01	254±26	33.85±0.01	283±17
34.44±0.02	366±42	34.40±0.02	431±38	34.46±0.01	574±25	34.46±0.01	516±14

the smooth fitted background under the Q_{ggg} peak in the gating region of the $^{9}Be(^{24}Mg,^{12}C^{16}O)^{5}He$ total energy spectrum. The subtraction of the estimated background results in the excitation energy spectrum shown in Fig. 7(d). This closely resembles the spectrum seen with the lithium target, with peaks observed at 28.2, 29.6, 30.5, 31.7, 33.2, 33.9, and 34.5 MeV (Table III).

The similarity noted between the excitation energy spectra for the three reactions appears to be enhanced by the ^{16}O fragment energy gating. Not only is the average difference in the measured centroids for the states listed in Table III reduced to 125 keV, but there is also a generally good agreement between the measured widths of the peaks. This strongly suggests that the same states are being populated in the different reactions. The lowest widths observed, of the order of 200–250 keV (depending on the target), are consistent with Monte Carlo predictions [10] of the excitation energy resolution. These simulations include the detector performance, the effects of interactions in the target and contributions from the reaction kinematics and beam resolution (see Table IV). The values predicted for the three targets range from a resolution of 240 keV for the carbon target to

TABLE IV. Contributions to the resolution in the reconstructed excitation energy spectrum as determined from a Monte Carlo simulation. Each effect is simulated individually. The total resolution predicted when all effects are simulated together is also shown.

Effect	^{12}C target contribution (keV)	^{7}Li target contribution (keV)	^{9}Be target contribution (keV)
Beam energy loss in target	<1	<1	<1
Beam energy spread	<1	<1	<1
Beam divergence	<1	<1	<1
Beam energy straggle in target	<1	<1	<1
Beam spot size	5	4	6
Detector telescope energy resolution	68	66	66
In-plane position resolution	103	105	104
Out-of-plane position resolution	125	132	131
Fragment energy loss in target	95	88	134
Fragment energy straggle in target	14	14	16
Fragment angular straggle in target	83	87	84
Fragment energy straggle in detector window	25	24	25
Fragment angular straggle in detector window	41	39	40
Fragment energy straggle in gas detector	34	34	34
Fragment angular straggle in gas detector	22	22	22
All effects simulated together	239	239	260

260 keV for the beryllium target. The errors associated with these values are expected to be of the order of 10%. The Monte Carlo results suggest that although the lower widths are likely to be limited by the experimental resolution, it is possible that either the natural widths of many of the wider states have been observed, or that they are multiplets.

A more complete comparison between the excitation energy spectra shown in Fig. 7 requires knowledge of the angular momenta of the states. From previous work only one tentative spin assignment exists, for the $J = (11)$ state at approximately 29.7 MeV in the $^{12}C(^{24}Mg,^{12}C^{16}O)^{8}Be$ channel [2]. Other work [3] found no structure in the angular correlations of the breakup fragments. This was also the case in the present work and can be attributed to two factors, as was also noted in the previous work [3]. First, the individual peaks lie upon a high level of background events which are present due to the significant underlying background included in the gate on the Q_{ggg} peak in the total energy spectrum. The width of this gate is determined by the total energy resolution. Monte Carlo simulations indicate that this is in turn is limited by the thickness of the targets used during the experiment to increase the breakup yield. Secondly, the density of states is expected to be relatively high for the $^{12}C + ^{16}O$ breakup of ^{28}Si, as suggested by the number of resonances seen in $^{12}C + ^{16}O$ scattering measurements [13,14]. In the $^{12}C(^{24}Mg,^{12}C^{12}C)^{12}C$ reaction, for which spin assignments have been made [8], the exit channel symmetry dictates that only states with even spin may be observed. In the $^{12}C + ^{16}O$ case, however, no such restriction applies, and it is possible to populate both even and odd spins. The observed resolution of ~ 250 keV in the excitation energy spectrum (see Tables III and IV) could easily be insufficient to resolve two neighboring states of even and odd (but similar) spins. In such cases, the structure in the angular correlation will be lost. In principle, a future experiment could improve the excitation energy resolution by means of improved angular resolution, requiring a much larger detector array. The $E_{\rm tot}$ resolution could also be improved by using thinner targets. which would further improve the excitation energy resolution (see Table IV). Thus, spin assignments may eventually become possible.

Although no spin assignments have been made for the states it is important to consider how the angular momentum matching for α transfer varies between the reactions on the three targets (^{12}C, ^{9}Be, and ^{7}Li). This has been estimated using the approach of Brink [22], wherein the overall goodness of matching has been calculated as a function of excitation energy, for each reaction, as described by Anyas-Weiss *et al.* [23]. For a given final spin in ^{28}Si, the functional form for the matching using ^{7}Li and ^{9}Be targets are almost identical, with the overall magnitude enhanced by a factor of approximately 2–4 for ^{7}Li. For the ^{12}C target, the curve closely resembles the ^{9}Be results in form and magnitude, but is shifted down in excitation energy by ~ 7 MeV. Representative calculations are shown in Fig. 8. Overall, the region of excitation for which the present experiment is optimized [$E_x(^{28}Si) = 27$–35 MeV] is best matched for α-transfer populating states with $\mathbf{J} = (11 \pm 3)$ for all three targets, with the matching for different spins almost identical

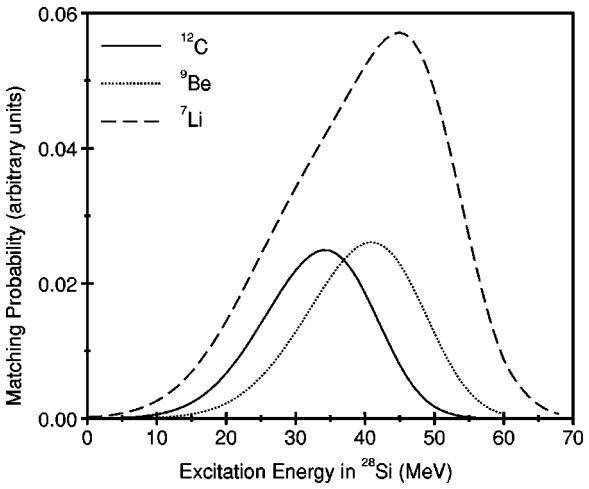

FIG. 8. Angular momentum matching probability for the (^{24}Mg,^{28}Si) reaction at 170 MeV, for α-cluster transfer to a $\mathbf{J} = 11$ state in ^{28}Si, using targets of ^{12}C,^{9}Be, and ^{7}Li.

in the case of ^{7}Li and ^{9}Be. This not only strengthens the inference drawn from the similar shapes of the ^{28}Si excitation energy spectra for the three targets, but also provides some support for the $\mathbf{J} = (11)$ assignment made for the state at ~ 29.7 MeV in the $^{12}C(^{24}Mg,^{12}C^{16}O)^{8}Be$ channel [2].

The double differential cross sections for reactions with the three targets (^{12}C,^{9}Be, and ^{7}Li), summarized in Table II, are directly measured quantities (in the laboratory frame). However, they are implicitly averaged across the detector acceptances, and as such are sensitive to the precise experimental geometry. A procedure to correct for the coincidence efficiency has been devised, based on the Monte Carlo simulations, to give an estimate of the total cross section for the ($^{24}Mg,^{12}C^{16}O$) reaction. To achieve this, each of the excitation energy spectra shown in Fig. 3 were corrected for coincidence efficiency (indicated by the dashed lines) on a channel-by-channel basis, and integrated over the excitation energy region 27–36 MeV which spans the observed structure. For each target, the background contribution to the excitation energy spectrum was estimated from the peak to background ratio in the gating region of the Q_{ggg} peak in the corresponding $E_{\rm tot}$ spectrum [shown in Figs. 1(a), 1(c), and 1(d) for the ^{12}C,^{7}Li, and ^{9}Be target data, respectively], and this was used to scale the integrated counts accordingly. The statistical errors were combined in quadrature with an additional uncertainty of 20% to account for relative variations in the angular distributions of the scattered $^{28}Si^{*}$ for different targets (the angular acceptance in terms of the ^{12}C-^{16}O breakup angle was typically 100°, which is sufficient to integrate over any structure in the breakup correlation). An additional estimated systematic error of up to 30% in the efficiency calculations, applicable to the absolute scaling for all targets, is shown separately. The total cross sections obtained using this procedure are included in Table II, and follow the same systematics as the double differential cross sections, namely that the ^{7}Li and ^{9}Be targets give values of order three times the ^{12}C target value.

Tanabe *et al.* [24] have studied the ($^{6}Li,d$) reaction on ^{24}Mg in normal kinematics and observed states in ^{28}Si up to

~ 20 MeV, above which the background rose significantly even at the quite high beam energy of 72.7 MeV. No significant breakup of ^{28}Si is expected for states below ~ 26 MeV (see Fig. 3 from the present experiment), because although the $^{12}C+^{16}O$ threshold occurs at 16.75 MeV, the Coulomb barrier of approximately 8.5 MeV inhibits low-energy breakup. Thus, the study of $^{12}C+^{16}O$ breakup states in a conventional $(^6Li,d)$ or $(^7Li,t)$ experiment is extremely challenging and inverse kinematics as used here offers many advantages.

IV. SUMMARY

A comparative study of the $^{12}C(^{24}Mg,^{12}C^{16}O)^8Be$, $^7Li(^{24}Mg,^{12}C^{16}O)t$, and $^9Be(^{24}Mg,^{12}C^{16}O)^5He$ reactions strongly suggests that the same excited states in ^{28}Si are populated in the three cases. An α-transfer process is identified as the most likely reaction mechanism populating the $^{12}C+^{16}O$ breakup states observed in ^{28}Si. This is consistent with the suggestion that the reactions are populating states associated with the prolate minimum in the Nilsson-Strutinsky potential energy surface of ^{28}Si, which has a four-particle–four-hole configuration. In order to extend the association between the states observed in the different reaction channels it is desirable that a higher resolution measurement be performed, with the aim of obtaining spin assignments. This would require the use of thinner targets and better detector resolution, implying a combined increase in coincidence efficiency and beam exposure. Carbon would be the best choice from the targets considered here, if the same techniques were to be employed. This is because there is very little contribution from background processes in the $^{12}C(^{24}Mg,^{12}C^{16}O)^8Be$ reaction, and because thin self-supporting carbon targets are readily available. This experimental advantage would easily compensate for the lower cross section measured for the ^{12}C target compared to ^7Li or ^9Be. In addition, the $\mathbf{J}^\pi=0^+$ ground states of ^{12}C and ^8Be should allow an angular correlation analysis to give more complete spin information [25]. Besides providing further tests of the proposed α-transfer mechanism, such a measurement would allow a detailed comparison with the $^{12}C+^{16}O$ scattering resonances, as has been successfully achieved in the $^{12}C+^{12}C$ channel [10]. It is also important to extend these measurements to $^{12}C+^{16}O$ breakup states observed via other entrance channels and hence populated via other mechanisms. The $^{12}C(^{20}Ne,^{12}C^{16}O)^4He$ and $^{16}O(^{16}O,^{12}C^{16}O)^4He$ reactions have previously been reported [4,6] and are thus candidates for further study. Further experiments may also include a comparative study of different decay channels to provide some measure of any enhancement above statistical, as has been applied to ^{24}Mg breakup [26].

ACKNOWLEDGMENTS

The authors would like to acknowledge the financial support of the Engineering and Physical Sciences Research Council (EPSRC). M.S., R.C., and G.D. would like to thank EPSRC for individual financial support. The cooperation and assistance of the staff of the 14UD accelerator facility at the Australian National University (ANU) is gratefully appreciated. This work was carried out under a formal collaboration agreement between EPSRC and ANU. The authors would also like to thank Dr. C. Jeynes of The University of Surrey Ion Beam Center for his work on the Rutherford back scattering analysis of the targets used.

[1] B.R. Fulton, S.J. Bennett, C.A. Ogilvie, J.S. Lilley, D.W. Banes, W.D.M. Rae, S.C. Allcock, R.R. Betts, and A.E. Smith, Phys. Lett. B **181**, 233 (1986).

[2] M. Freer, in Probing Cluster Structures Through Breakup Reactions, Proceedings of the 6th International Conference on Clusters in Nuclear Structure and Dynamics, Strasbourg, 1994 (unpublished), p. 29

[3] N. Curtis, Ph.D. thesis, University of Birmingham, 1995.

[4] J.T. Murgatroyd, S.J. Bennett, B.R. Fulton, J.S. Pople, N.S. Jarvis, D.L. Watson, W.D.M. Rae, Y. Chan, D. DiGregorio, J. Scarpaci, J. Suro Perez, and R.G. Stokstad, Phys. Rev. C **51**, 2230 (1995).

[5] S.J. Bennett, M. Freer, B.R. Fulton, J.T. Murgatroyd, P.J. Woods, S.C. Allcock, W.D.M. Rae, A.E. Smith, J.S. Lilley, and R.R. Betts, Nucl. Phys. **A534**, 445 (1991).

[6] M. Freer, N.M. Clarke, R.A. Le Marechal, G. Tungate, R.P. Ward, and W.D.M. Rae, Phys. Rev. C **51**, 3174 (1995).

[7] N. Curtis, A.St.J. Murphy, M.J. Leddy, J.S. Pople, N.M. Clarke, M. Freer, B.R. Fulton, S.J. Hall, G. Tungate, R.P. Ward, S.M. Singer, W.N. Catford, G.J. Gyapong, R.A. Cunningham, J.S. Lilley, S.P.G. Chappell, S.P. Fox, C.D. Jones, D.L. Watson, P.M. Simmons, R.A. Hunt, A.C. Merchant, A.E. Smith, W.D.M. Rae, and J. Zhang, Nucl. Instrum. Methods Phys. Res. A **351**, 359 (1994).

[8] B.R. Fulton, S.J. Bennett, M. Freer, J.T. Murgatroyd, G.J. Gyapong, N.S. Jarvis, C.D. Jones, D.L. Watson, J.D. Brown, W.D.M. Rae, A.E. Smith, and J.S. Lilley, Phys. Lett. B **267**, 325 (1991).

[9] N. Curtis, A.St.J. Murphy, N.M. Clarke, M. Freer, B.R. Fulton, S.J. Hall, M.J. Leddy, J.S. Pople, G. Tungate, R.P. Ward, W.N. Catford, G.J. Gyapong, S.M. Singer, S.P.G. Chappell, S.P. Fox, C.D. Jones, D.L. Watson, W.D.M. Rae, P.M. Simmons, and P.H. Regan, Phys. Rev. C **53**, 1804 (1996).

[10] N. Curtis, N.M. Clarke, B.R. Fulton, S.J. Hall, M.J. Leddy, A.St.J. Murphy, J.S. Pople, R.P. Ward, W.N. Catford, G.J. Gyapong, S.M. Singer, S.P.G. Chappell, S.P. Fox, C.D. Jones, D.L. Watson, W.D.M. Rae, and P.M. Simmons, Phys. Rev. C **51**, 1554 (1995).

[11] G. Leander and S.E. Larsson, Nucl. Phys. **A239**, 93 (1975).

[12] J. Zhang, W.D.M. Rae, and A.C. Merchant, Nucl. Phys. **A575**, 61 (1994).

[13] N. Cindro, Riv. Nuovo Cimento **4**, 1 (1981).

[14] N. Cindro, Ann. Phys. (Paris) **13**, 289 (1988).

[15] M. Harvey, in Many Nucleon Correlations in Light Nuclei,

Proceedings of the 2nd International Conference on Clustering Phenomena in Nuclei, College Park, Maryland, 1975 (unpublished), p. 549
[16] M.V. Mihailović and M. Poljšak, Nucl. Phys. **A311**, 377 (1978).
[17] J. Hiura and R. Tamagaki, Prog. Theor. Phys. Suppl. **52**, 25 (1972).
[18] K.S. Krane, in *Introductory Nuclear Physics* (Wiley, New York, 1988), Chap. 20, p. 797–799
[19] J.T. Murgatroyd, J.S. Pople, N.M. Clarke, B.R. Fulton, M.J. Leddy, W.N. Catford, S.P. Fox, G.J. Gyapong, C.D. Jones, D.L. Watson, W.D.M. Rae, Y. Chan, R.G. Stokstad, and S.J. Bennett, Phys. Rev. C **58**, 1569 (1998).
[20] C.L. Woods, F.C. Barker, W.N. Catford, L.K. Fifield, and N.A. Orr, Aust. J. Phys. **41**, 525 (1988).
[21] C. Lee, D.D. Caussyn, N.R. Fletcher, D.L. Gay, M.B. Hopson, J.A. Liendo, S.H. Myers, M.A. Tiede, and J.W. Baker, Phys. Rev. C **58**, 1005 (1998).
[22] D.M. Brink, Phys. Lett. **40B**, 37 (1972).
[23] N. Anyas-Weiss, J.C. Cornell, P.S. Fisher, P.N. Hudson, A. Menchaca-Rocha, D.J. Millener, A.D. Panagiotou, D.K. Scott, D. Strottman, D.M. Brink, B. Buck, P.J. Ellis, and T. Engeland, Phys. Rep. **12**, 201 (1974).
[24] T. Tanabe, K. Haga, M. Yasue, K. Sato, K. Ogino, Y. Kadota, M. Tochi, K. Makino, T. Kitahara, and T. Shiba, Nucl. Phys. **A399**, 241 (1983).
[25] S. Marsh and W.D.M. Rae, Phys. Lett. **153B**, 21 (1985).
[26] M. Freer, N.M. Clarke, B.R. Fulton, J.T. Murgatroyd, A.St.J. Murphy, S.P.G. Chappell, R.L. Cowin, G. Dillon, D.L. Watson, W.N. Catford, N. Curtis, M. Shawcross, and V.F.E. Pucknell, Phys. Rev. C **57**, 1277 (1998).